Unimolecular Dissociation Rate Constants: Chlorobenzene Cations Revisited by Using a New Method

R. J. Stanley, M. Cook, and A. W. Castleman, Jr.*

Department of Chemistry, The Pennsylvania State University, University Park, Pennsylvania 16802

(Received: October 10, 1989)

Unimolecular dissociation rates of metastable molecular ions formed at the laser focus of a time-of-flight mass spectrometer (TOFMS) have been determined by measuring the relative concentrations of "parent" metastable ions and the "daughter" fragment ions as a function of their retained kinetic energies upon dissociation. This is accomplished by the use of a simple one-stage ion mirror/energy analyzer. For a given reflection potential on the ion mirror, only those ions with a kinetic energy equal to or less than the reflection potential are detected. In this way, the relative concentrations of the parent and daughter ions as a function of their position of dissociation in the time-of-flight (TOF) lens can be measured, and consequently the dissociation lifetime can be derived. This technique has been applied to measuring the unimolecular dissociation rate of chlorobenzene ion ($C_6H_5Cl^+$) in the three-photon energy range of 13.64–13.92 eV through resonance-enhanced two-photon state-selected ionization of chlorobenzene in a supersonic molecular jet. The method demonstrates a minimum dynamic range of 10^5 to 2×10^7 s^{-1} and is in good agreement with previous work. The data suggest that rotational temperature plays a role in the unimolecular dissociation lifetime of the metastable ions.

Introduction

Understanding the metastability of excited molecular ions in the gas phase has a bearing on the number of disciplines including atmospheric and environmental science and radiation and combustion chemistry and also further contributes to a basic understanding of how excess energy, retained upon ionization, is redistributed into the various parts of the ion. Measurement of the rates of metastable ion dissociation has been the object of much attention, and various techniques have been developed and employed in such studies. For example, Baer et al.[1] have used the photoion–photoelectron coincidence technique (PIPECO) to study the unimolecular dissociation of halobenzene ions. The rate constant, $k(E)$, was obtained by an analysis of the daughter ion time-of-flight distribution in coincidence with zero kinetic energy electrons produced by irradiation of the sample with vacuum-UV light. In other work Rosenstock et al.[2] have studied chlorobenzene metastability through the analysis of "breakdown curves", where the concentration of the daughter ion was monitored by pulsing the ion extraction grids in their PIPECO apparatus. More recently, Durant et al.[3] have investigated the dissociation of state-selected chlorobenzene ions prepared using multiphoton ionization (MPI). The internal energy of the ions was monitored by a photoelectron spectrometer, and the rate of dissociation of the excited molecular ions was derived from the analysis of their asymmetric time-of-flight "tail" in a time-of-flight mass spectrometer. Another method of investigating the unimolecular decomposition of ions includes one employed by Neusser et al.,[4a] who used a reflection mass spectrometer to separate parent and daughter ions in order to study the dissociation of benzene and aniline cation metastables in the drift region of a TOF mass spectrometer. Using ion cyclotron resonance spectroscopy, Dunbar has also measured metastability in $C_6H_5Cl^+$.[5] Building on the electron impact ionization work of Hertel and Ottinger,[6a] Andlauer and Ottinger[6b] performed dissociation rate measurements in which molecules were ionized by charge transfer with Xe^+, Ar^+, Kr^+, CO^+, and N_2^+ ions. Following ionization the ions were accelerated through a single-stage electric field, mass selected by a quadrupole mass filter, and finally energy analyzed by an electric sector device. While his technique has some formal resemblance to the technique described herein, the measurement and analysis differ in several crucial ways, as will be discussed below.

With the exception of the technique of Neusser et al.,[4a] all of the above methods rely on some type of time-of-flight distribution analysis to determine $k(E)$. That is, each ion pulse has a different arrival time at the detector that depends on its initial spread in kinetic energy, its "birth potential" (the potential, relative to ground, at the point of ionization), and the spread in energies caused by the ionization technique (laser spot size, vacuum-UV beam diameter, electron beam diameter, etc.). Consequently, the asymmetric mass peak distribution that results from a delayed dissociation process is convoluted with the instrument line-shape function. The instrument function itself can contribute only to a broadening of the TOF tail, thereby leading to the necessity of determining the line-width function and mathematically deconvoluting it from the data before an accurate rate constant can be calculated. This problem has been handled in several ways and will be discussed in more detail later.

Neusser et al.[4a] arrived at a $k(E)$ by measuring the concentrations of parent and daughter ions using a reflectron to separate the daughters that are often buried beneath the much larger parent peak. By calculating the drift time from the TOF lens to the reflectron, they have deduced the metastable rate constants for benzene and aniline. Because they measure the daughter ion intensity in the drift region of the TOFMS, they are not able to look at dissociation reactions that are basically completed before the metastables leave the TOF lens, i.e., characteristic dissociation times near or greater than 10^{-7} s. Recently, Neusser has demonstrated this technique using angular momentum selected ions.[4b]

We present here a new technique for the measurement of molecular ion metastable rate constants that can span a range from 10^4 to 2×10^7 s^{-1} in a MPI-TOFMS that is independent of the time-of-flight distribution of the metastable daughter ion peak. In this method, a single-stage ion mirror is used to energy analyze ions produced in the first acceleration region of our TOFMS. As we shall show, the kinetic energy acquired by the daughter ion is a consequence of its lifetime as a metastable parent ion. By measuring the integrated ion intensity of metastable ions versus their kinetic energies and mapping this energy back into time, we can measure rate constants that are relatively insensitive to the broadening of the TOF peak distribution function caused by convolution of the TOF ion peak with the instrument line function. Any such effects would show up as a nonlinearity in

---

[1] Baer, T.; Tsai, B. P.; Smith, D.; Murray, P. T. *J. Chem. Phys.* **1976**, *64*, 2460.

[2] Rosenstock, H. M.; Stockbauer, R.; Parr, A. C. *J. Chem. Phys.* **1979**, *71*, 3708.

[3] Durant, J. L.; Rider, D. M.; Anderson, S. L.; Proch, F. D.; Zare, R. N. *J. Chem. Phys.* **1984**, *80*, 1817.

[4] (a) Neusser, H. J.; Kühlewind, H.; Boesl, U.; Schlag, E. W. *Ber. Bunsen-Ges. Phys. Chem.* **1985**, *89*, 276. (b) Neusser, H. J. *J. Phys. Chem.* **1989**, *93*, 3897.

[5] Dunbar, R. C. *J. Am. Chem. Soc.* **1989**, *111*, 5572.

[6] (a) Hertel, I.; Ottinger, Ch. *Z. Naturforsch.* **1967**, *22a*, 1141. (b) Andlauer, B.; Ottinger, C. *Z. Naturforsch.* **1972**, *27*, 293.

0022-3654/90/2094-3668$02.50/0

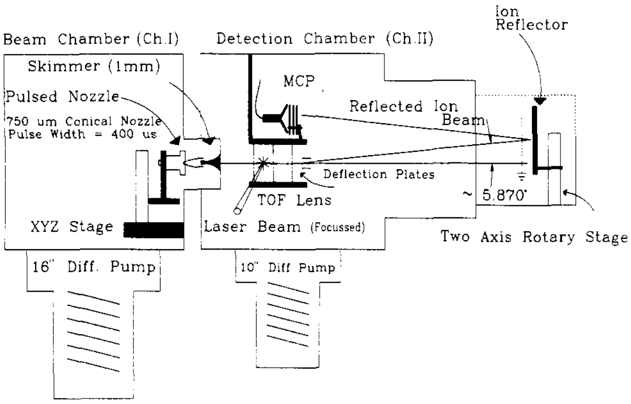

Figure 1. Time-of-flight mass spectrometer: energy analyzer. The pulsed nozzle in the beam chamber produces <400-μs pulses through a 750-μm conical orifice at 10 Hz. The gas mixture is 0.8% chlorobenzene in helium buffer gas at 1000 Torr. The pressure in the beam chamber is $<10^{-5}$ Torr. The molecular jet is skimmed by a 1-mm skimmer and crosses the focused laser beam between the grids of the TOF lens. The pressure in chamber II is $\sim 2 \times 10^{-6}$ Torr. The ions are accelerated and deflected toward the ion mirror at the rear of the detection chamber. Only those ions with a kinetic energy equal to or less than the applied reflection potential will be detected at the ion multiplier.

the data analysis, assuming a first-order rate process (see Theory and Analysis). The method has the further advantage in that noise peaks (any nonmetastable mass peak) are of no consequence to the rate determination, even if they reside directly on top of the signal of interest. We have chosen the dissociation of state-selected chlorobenzene ions as a test case because there already exists a fairly substantial number of measurements for comparison.

Experimental Section

The laser ionization molecular beam time-of-flight mass spectrometer, housed in two differentially pumped chambers, is shown schematically in Figure 1. The beam chamber, which contains the pulsed nozzle, is pumped by a 16-in. diffusion pump with a (baffled) throughput of ~4000 L/s. The pulsed nozzle is a General Valve Series 9 equipped with a 750-μm conical orifice and mounted coaxially with the TOF ion beam axis. The pulsed nozzle is overdriven to give a pulsed beam of ~400-μs duration. The pressure in the chamber during operation with 1000–2000 Torr of gas, mainly He, is typically 6×10^{-6} Torr. The molecular beam is skimmed by a Beam Dynamics 1-mm skimmer which separates the beam and TOFMS chambers. The nozzle-skimmer distance is 2 cm. The pulsed nozzle is mounted on a translation stage that allows the nozzle to skimmer, and consequently the nozzle-interaction distance, to be varied. This allows us to measure the neutral molecular beam velocity by delaying the laser with respect to the pulsed nozzle beam and mapping out the neutral beam profile at different nozzle to interaction region distances.

The TOF spectrometer is located in a chamber pumped by a 10-in. diffusion pump equipped with a liquid nitrogen baffle. The pressure in this chamber never exceeds 4×10^{-6} Torr. The time-of-flight lens is mounted such that the skimmer-interaction region distance is ~8 cm. The TOF lens consists of three circular plates of 7.6-cm diameter, with 1.3-cm holes (see Figure 2), spanned by 95% transmittance Ni grids. Lenses 1 and 2 define the interaction and first acceleration regions of the TOF lens and are separated by a distance of 1.1 cm. Lens 1 is set at a potential U_1 and lens 2 at U_2, the second acceleration region is 1.0 cm in length, and the last element of the TOF lens is grounded. The field gradient in the first region is typically 150 V/cm, and 1100 V/cm in the second. The ion beam is deflected ~6° with a set of deflection plates.

The ion mirror–energy analyzer consists of stainless steel ground and reflector plates separated by a distance of 1.75 cm, located 52 cm from the interaction region and 5 cm off of the neutral beam axis. The ground plate is covered with a Ni wire mesh. The reflector is a cylindrical element, the back plate of which is highly polished to ensure that surface irregularities do not lead to scattering of ions whose energy allows them to nearly sample the potential before being reflected. The reflectron potential is supplied by a computer-controlled programmable power supply, which has a resolution of 0.2 V.

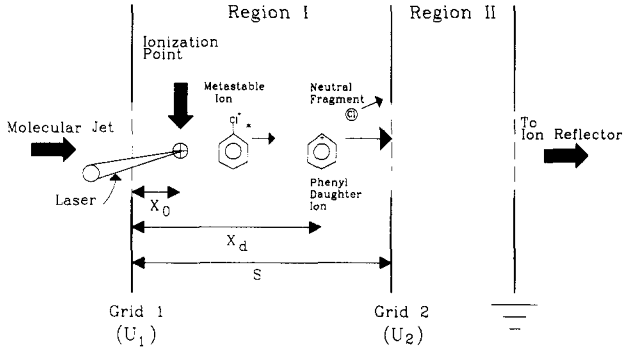

Definitions: X0 = Point of ionization relative to Grid 1
Xd = Point of metastable dissociation
S = Gap between Grids 1 and 2

Figure 2. Time-of-flight lens geometry. This cartoon of the TOF lens shows the nature of the fragmentation process of the metastable $C_6H_5Cl^+$ ion. It should be noted that the neutral beam contributes some kinetic energy to the ion, but this turns out to be of secondary importance. What is most relevant is that at the point of dissociation, x_d, the daughter ion has only that fraction of the kinetic energy of the parent ion corresponding to the mass ratio of the daughter to parent mass. Also note that ions "born" at the laser focus that do not dissociate in the time of flight to the multiplier have the full kinetic energy, U_0. The potentials are nominally $U_1 = 1250$ V, $U_2 = 1100$ V. With $s = 1.1$ cm, this leads to a 135 V/cm field gradient in region 1. The field in region 2 was 1100 V/cm. The acceleration field was varied, but no change in the measured rate constants was observed.

The ions that are reflected from the ion mirror are detected by a 2.54 cm diameter chevron microchannel plate (MCP—Galileo FTD 2003) that has a gain of 10^7 and a rise time of 2 ns. The MCP is mounted directly above the TOF lens for a total "drift" distance of ~104 cm.

The laser system consists of a Quanta Ray DCR-1A Nd^{3+}:YAG pump laser, whose output is frequency doubled to 532 nm with KDP; it is used for pumping a dye laser (QR PDL2) using coumarin 500 (Exciton). The second harmonic (SHG) of the dye is obtained with another KDP crystal, and the resultant UV light is separated from the dye laser light by using a UV-transmitting filter. When wavelength scans are performed, the SHG crystal is automatically tracked (Quanta Ray WEX-1). The UV beam, which has a 5–7-ns duration, is focused on the molecular beam by using a 50-cm suprasil lens. Beam fluctuations are monitored on a shot-to-shot basis with a fast joulemeter (Molectron J3-02) sample and hold circuit that provides a dc signal to one of the A/D inputs of the computer/data acquisition system described below.

The TOF signal from the MCP is fed directly into a 100-MHz 2K channel 8-bit resolution digital storage oscilloscope (DSO—Biomation 4500), which is triggered by a fast photodiode. The DSO is capable of averaging up to 256 shots, but by interfacing the DSO to our lab computer, we are able to perform virtually unlimited signal averaging. The DSO is under computer control and is recalibrated by the computer after each accumulation.

The coordination of the various subsystems is controlled by a master clock, which provides start pulses to the laser and a variable delay generator (Mech-Tronics four-phase delay) which triggers the pulsed nozzle. The computer is capable of providing a programmable trigger to the pulsed nozzle, allowing the neutral beam profile to be mapped out.

A 8086-2 8-MHz microcomputer, programmed in Turbo Pascal, is used to control the experiments described below. The program is interrupt driven and has completely automated the data collection and analysis in our laboratory. Up to four voltages may be monitored and stored with 12-bit accuracy (IBM DACA board). Laser power measurements are made on a shot-to-shot basis. The backing pressure of the pulsed nozzle and the pressures in the two chambers are recorded at these times as well. Timing operations, such as a scan of the molecular beam profile, are performed by an 8254 chip on the DASH-8 card (Metrabyte).

The DACA board also controls the energy analyzer through the use of its 12-bit D/A converter. The 0–10-V D/A output is fed into a precision voltage divider that drives the voltage programmable input (0 to –5 V) to the reflector power supply (Bertran 313A). The voltage is measured with a Keithley DVM Model 177 with a Fluke HV probe. The computer-controlled energy analyzer is stable to within 0.1 V. A calibration is made on the energy analyzer to ensure linearity before each run.

Theory and Analysis

In a time-of-flight (TOF) mass spectrometer, all ions that travel intact through the acceleration region have the same kinetic energy (KE), q times the potential at the point of ionization (birth potential, U_0). An ion that dissociates in the acceleration region (dissociation daughter) ends up with a lower KE, which is a function of the distance traveled between ionization and dissociation; this is due to the fact that the neutral fragment carries off a constant proportion of the KE that the ion has acquired by the time it dissociates. Thus, if the kinetic energy of a particular ion in the flight region is known, the time between ionization and dissociation (time of reaction, t_r) for that ion can be calculated.

In our method, we increment the voltage on the ion mirror, starting well below the birth potential, and take an accumulated mass spectrum at each voltage. Each mass spectrum contains signal from only those ions with kinetic energies less than q times the reflector potential, i.e., ions that dissociated after the characteristic time, t_r, for that potential. Ions that dissociate earlier, having higher KE, pass "through" the mirror without being detected. The rate constant is determined by plotting the natural logarithm of the integrated ion signal of the daughter ion versus the t_r calculated for each reflector potential; the slope, k, is the unimolecular rate constant for that dissociation reaction.

In the case where the dissociation process can be modeled by a first-order rate law, then

$$\mathrm{d}P(t)/\mathrm{d}t = -kP \tag{1}$$

where $P(t)$ is the number of parent ions at any time t that have yet to undergo unimolecular dissociation. Integration of this equation yields the familiar expression

$$P(t) = P_0 e^{-kt} \tag{2}$$

where P_0 is the number of parent ions (for this reaction pathway) at $t = 0$. Since $D_\infty - D(t) = P(t)$, where D_∞ is the number of daughter ions at infinite time ($D_\infty = P_0$), we can rewrite eq 2 as

$$D(t)/D_\infty = 1 - e^{-kt} \tag{3}$$

The ratio on the left-hand side of eq 3 represents the fraction of parent ions that have dissociated by time t in terms of the concentration of the daughter ion, D. However, the ion mirror reflects all ions having a kinetic energy less than qU_r, where U_r is the potential applied to the back element of the ion mirror; consequently, the daughter ions that are detected are the fraction that already have dissociated at t_r for that potential. Thus, the TOF spectrum at a particular U_r contains the fraction of parent that remains at t_r:

$$1 - D(t)/D_\infty = e^{-kt} \tag{4}$$

This is shown graphically in Figure 3, which is a plot of the chlorobenzene parent and daughter TOF spectra for various reflection potentials. It can be seen clearly that the chlorobenzene parent peak dies out below the reflection potential corresponding to the potential at the point of ionization (within the range of potentials defined by the laser spot size), but that the daughter peak has significant intensity corresponding to much lower kinetic energies. The daughter ion signal is integrated as a function of reflection potential. The problem then becomes one of finding a "mapping" equation that relates the reflection potential to the metastable lifetime of the parent ion.

For nondissociating ions born a distance x_0 from lens 1, the drift-region energy, qU_0, can be expressed as

$$qU_0 = q[U_1 - (U_1 - U_2)x_0/s] + M_p v_0^2/2 \tag{5}$$

where M_p is the parent mass, s is the distance between lens 1 and lens 2 (1.1 cm in the present experimental setup), and q is 1.6012 × 10^{-12} coulombs (this value of q makes volts compatible with CGS units). The initial kinetic energy due to the molecular beam velocity, v_0, is explicitly taken into account. The value of x_0 is obtained experimentally from the measured cutoff potential of the parent peak.

If a metastable ion travels some distance x_d before dissociating, the kinetic energy of the daughter ion at the point of dissociation is merely the kinetic energy the parent ion has acquired falling a distance x_d through the field gradient of the first acceleration region, times the ratio of the final to initial mass:

$$qU_d = (qE_1(x_d - x_0) + M_p v_0^2/2)M_r \tag{6}$$

where $E_1 = (U_1 - U_2)/s$ and $M_r = M_d/M_p$. The kinetic energy of the daughter ion in the drift region is just that from eq 6 plus that energy acquired from acceleration in the remainder of field 1 and the whole of field 2:

$$\mathrm{KE}_d = q[U_d + (s - x_d)E_1 + U_2] \tag{7}$$

Since the reflection occurs at a small angle with respect to the normal, we must include this angle in eq 7 to obtain the reflection potential, U_r, which is necessary to turn an ion of energy KE_d back toward the ion multiplier:

$$qU_r = q\cos^2\phi[U_d + (s - x_d)E_1 + U_2] \tag{8}$$

The previous equation can be rearranged to obtain an expression for the position of dissociation:

$$x_d = s - [U_r/\cos^2\phi - U_d - U_2]/E_1 \tag{9}$$

We now need only determine how x_d is mapped into the metastable lifetime.

The kinetic energy the parent gains traversing x_d is just

$$M_p v^2(x_d)/2 = qE_1 x_d + M_p v_0^2/2 \tag{10}$$

Thus, its velocity as a function of distance in the TOF lens, x_d', is

$$v(x_d') = (2qE_1 x_d'/M_p + v_0^2)^{1/2} \tag{11}$$

However,

$$t_d = x_d'/v(x_d') \tag{12}$$

so that the time of dissociation t_d for a particular x_d (which is determined by the energy analysis) is found by integrating out the time dependence in eq 12:

$$t_d = \int_0^{x_d} \mathrm{d}x_d'/v(x_d') \tag{13}$$

$$t_d = (M_p^{1/2}/qE_1)[(2qE_1 x_d + M_p v_0^2)^{1/2} - (M_p v_0^2)^{1/2}] \tag{14}$$

The equation that maps the measured kinetic energy of the dissociation daughter ion into its time to dissociation is found by substituting x_d from eq 9 into eq 14. Figure 4a shows the integrated parent ion intensity versus reflection potential for the chlorobenzene ion, corrected for laser power fluctuations. The midpoint of the quasi-step function is taken to be the birth potential of the parent, U_0. Figure 4b shows the integrated daughter plus parent ion intensity versus reflection potential. The metastable contribution to the energy analysis at reflection potentials lower than the birth potential of the $C_6H_5Cl^+$ ion is clearly evident. A plot of the natural log of the ion intensity versus t_d is shown in Figure 5. The linearity of the data from 0.4 to 0.9 μs clearly shows that the dissociation of $C_6H_5Cl^+$ is a first-order process. Durant et al.[3] have also observed this to be a first-order decay process. The deviation from linearity at times <0.4 μs is attributed to the prompt ion signal feeding down into the metastable ion signal. Since the rate constant analysis is valid only in the linear region, this is of little consequence.

An energy analysis experiment is performed as follows. The programmable power supply is calibrated by using the digital

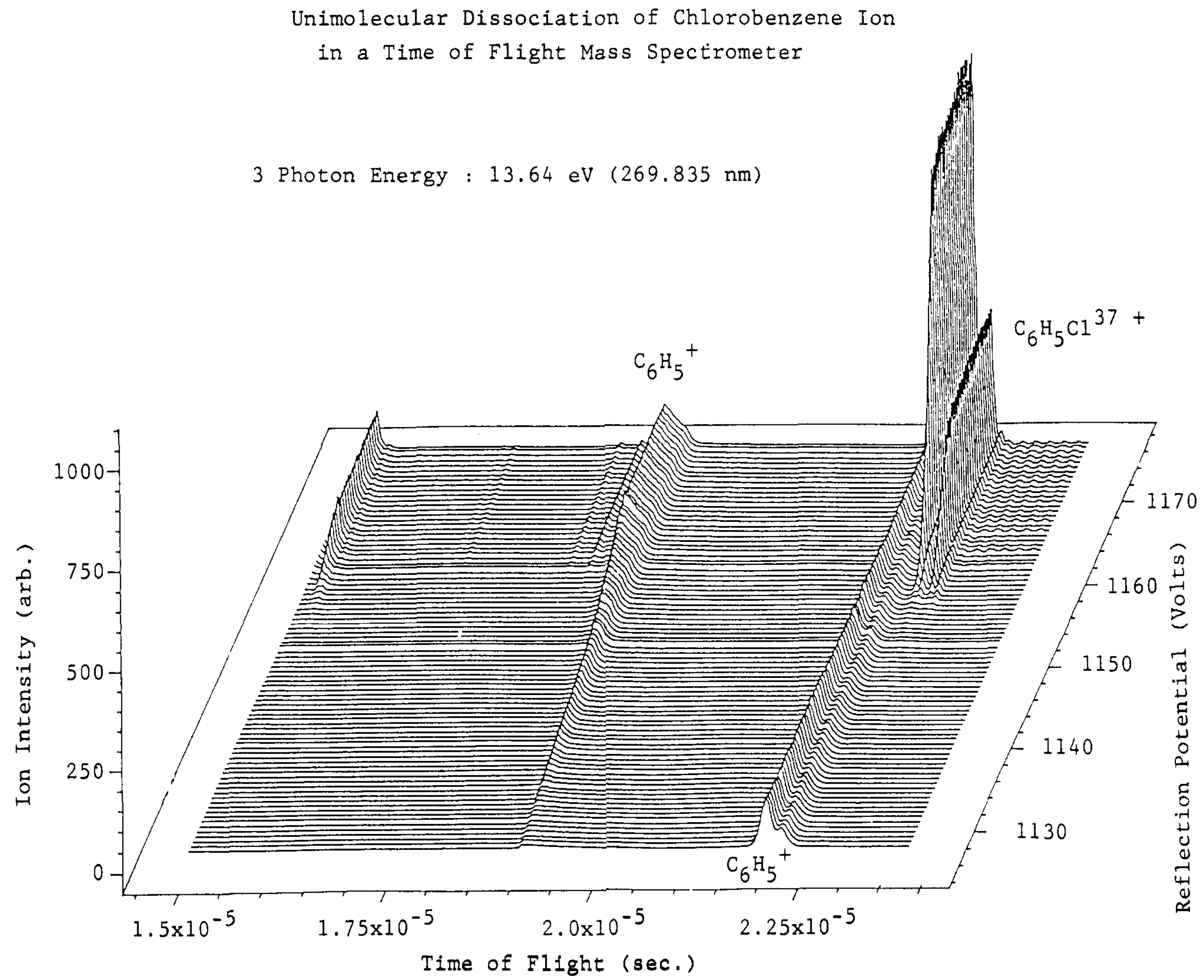

Figure 3. 3-D plot of the ion intensity as functions of the reflection potential and time of flight for a laser wavelength of 269.835 nm. It is clearly seen that at lower reflection potentials, only the phenyl daughter ion and the drift region daughters are visible. At that reflection potential that corresponds to the laser focus position, there is a dramatic increase in the ion intensity as the nondissociating parent ions appear. It can also be seen that any interfering peaks, as long as they are not metastable, will have no effect on this method, even if the contaminating ion sits on top of the daughter ion of interest. The analysis begins by integrating the ion intensity over the entire parent-to-daughter time of flight. Thus, the analysis becomes independent of the time of flight distribution.

voltmeter. First, a rough approximation of the birth potential of $C_6H_5Cl^+$ is made by manually varying the reflector potential. This establishes the limits of the energy analysis scan. The computer is programmed for the step size and lower and upper voltage limits of the scan, as well as the signal-averaging parameters under computer control. Each TOF mass spectrum of $C_6H_5Cl^+$ (mass 112.5 amu) and its daughter ion $C_6H_5^+$ (mass 77 amu) at a particular reflection potential are stored on the hard disk. At the end of the scan we then have a three-dimensional database of ion intensity versus time-of-flight of the ions and versus reflection potential.

During the writing of this paper, it was brought to our attention that Andlauer and Ottinger[6b] performed an experiment in which molecules were ionized by charge transfer, accelerated through a single-stage electric field, mass selected by a quadrupole, and energy analyzed by an electric sector. Their data analysis assumed a distribution of rate constants for the dissociation, and, indeed, these distributions were seen which showed discrete maxima. The ions used for charge transfer led to several different but discrete recombination energies, which vary in relative abundance. For example, Kr^+ gave two distinct energies for $Kr^+(^2P_{3/2})$ and $Kr^+(^2P_{1/2})$ of 14.0 and 14.67 eV, respectively. When these ions recombine with the target molecule (C_6H_5CN, C_6H_6, C_4H_4S), the internal energy of the product ions reflected the distribution of the ion used for charge transfer. Thus, the obtained rates must be deconvoluted for this effect. Our experiment would not be expected to show such a range of rates, since by multiphoton ionization we generate state selected ions. Further, since we plot ln I versus t, the existence of multiple rates would be apparent as a nonlinearity of the data, which is not seen (see Figure 5). The deviation seen at 0.4 μs is caused by the first traces of the parent peak, which begins to appear at this voltage due to the spread of birth potential(s).

Results and Discussion

UV excitation spectra were obtained prior to the energy analysis to assess the beam temperature and to locate the resonant (1 + 1) transitions. The results of the excitation spectra are in agreement with those obtained by Durant et al.[3] Vibrational hot bands, which would be indicative of a nonnegligible internal energy of the neutral molecule, were found to be about one-sixth as prominent as transitions from the vibrationless ground state. No further vibrational cooling was observed to be obtained at backing pressures above 1000 Torr. The rate constants were determined to be invariant within experimental accuracy for values ranging from 800 to 2000 Torr. Thus, any contributions from hot band excitation appears to be negligible.

Rate constants from 0_0^0 ($S_1 \leftarrow S_0$) transition (13.64 eV) up through ionizing energies of 13.95 eV were found to be invariant with laser fluence and focusing conditions, over a wide range, in agreement with Durant et al.[3] This indicates that only one metastable channel is being opened, since secondary metastable

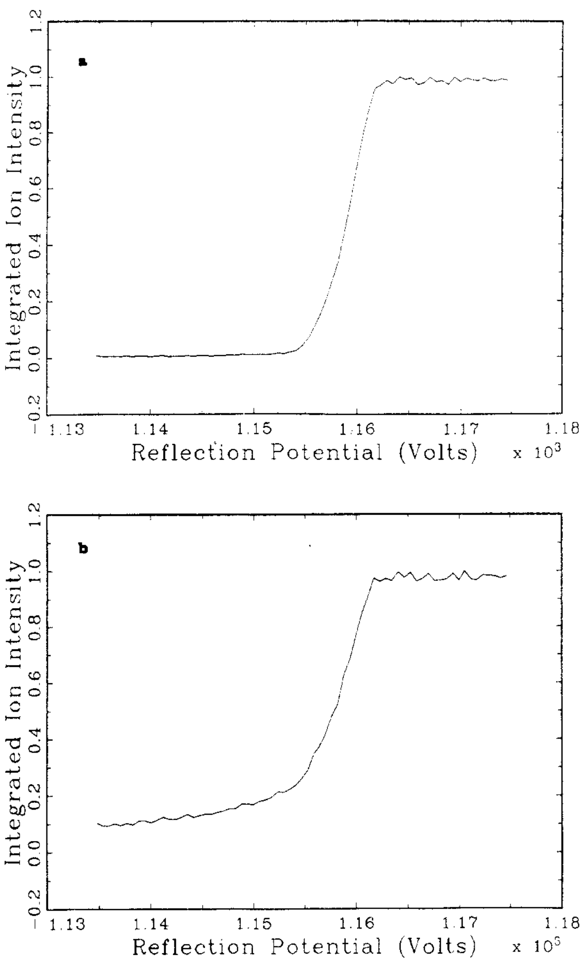

Figure 4. Parent and daughter ion energy analysis. (a) The integrated parent ion signal is plotted versus reflection potentials to yield this "transmission curve" at 268.005 nm. The width of the step (7.6 V) would be the result of a 620-μm laser spot size, though we estimate that the spot size should be around 300 μm. The broadening of this step could be the result of vibration of the apparatus relative to the laser beam, or possible scattering due to the ion mirror ground grid. The birth potential, U_0 = 1160.0 V, found by differentiating this cure, is used to calculate the position of ionization. (b) The parent plus daughter transmission curve. The rising integrated ion signal at low reflection potentials is indicative of metastable dissociation in the first acceleration region. The rate constant is contained in the part of the curve that is below U_0. The analysis is performed up to U_0 minus the parent ion step width.

processes would have led to deviations in the observed rate constants as a function of laser fluence.

The unimolecular dissociation rate constant for $C_6H_5Cl^+$ over the three-photon energy range of 13.64–13.95 eV is shown in Figure 6. To properly account for the internal energy of the metastable ions, the kinetic energy of the photoelectron must be known. Anderson et al.[7] have measured these energies for the chlorobenzene ion using a laser ionization TOF photoelectron energy spectrometer for the wavelengths used in this study. The photoelectron spectra showed that the vibrational energy of the ion depends upon the resonant intermediate state of the neutral. Even so, ions produced from the same vibronic S_1 neutral intermediate state gave a characteristic vibrational ion photoelectron spectrum with the exception of the 0^0_0 transition, which gave a single sharp peak. Thus, for a particular excitation, progressions involving the S_1 vibronic intermediate were observed, as well as, to a lesser extent, those of other vibrations. The authors suggested that a combination of selection rules and Franck–Condon factors determine the observed distribution.[7] The width of the vibrational distribution was <0.15 eV.

Durant[8] averaged over the observed photoelectron distribution to obtain an average photoelectron energy for a particular $S_1 \leftarrow S_0$ transition. The corrected three-photon energy is thus the total three-photon energy minus the average photoelectron energy for that particular wavelength. Also plotted are the RRKM best-fit values for model 1 of Rosenstock et al.,[2] which involves for the transition state of the ion a 23% reduction of all vibrational frequencies, and the relevant data from the TOF tail analysis method of Durant et al.[3] The agreement with the findings reported by Durant et al. is good in form, though an offset to higher rates is apparent in this work. Both MPI studies differ from the work of Rosenstock et al.

There are several factors that would affect the results obtained and the viability of the new technique presented herein. These involve the spread in birth potential in the TOF lens, collision-induced dissociation, and any smearing of the transmission curve introduced by the energy analyzer itself. It should be noted that the technique is suitable only where the mass range between the metastable peak of interest and the parent peak contains no other metastable contribution (or that it is very small or well separated).

The spread in ion birth potentials that occurs in the TOF lens is the convolution of several factors, if we neglect the initial kinetic energy spread of the neutral molecular beam, which our calculations indicate is negligible. The most obvious of these is the laser spot size, which is difficult to determine directly. Perhaps the most effective way of ensuring the minimum spot size, thus reducing the spread in birth potentials, is to maximize the amount of fragmentation, which is an indication of a maximum power density in the interaction region. This procedure is easily carried out by viewing the ion signal and its fragmentation pattern directly with an oscilloscope. Another factor that would smear out spread in birth potentials would be any displacement of the laser spot relative to the TOF grids, i.e., machine vibration relative to the laser beam. If we assume a 150 V/cm field in the interaction region, with a uniform laser spot size of 200 μm, a vibration-free apparatus would produce an energy spread of only 3 V. Introducing a 0.2-mm amplitude vibration between the focused laser and the TOF interaction region would broaden this energy spread to 9 V, which is what is observed in this study. Thus, it can be seen that vibration is a critical parameter and perhaps produces the ultimate limit on the kinetic energy spread in the TOF lens.

While the agreement in shape between Durant et al. and our data is quite good, the apparent offset in our data indicates that other processes might be contributing to the production of metastable ions. Collision-induced activation of prompt parent ions with neutral beam molecules as the ions are accelerated out of the TOF lens cannot be discounted.

The energy analyzer will also broaden the energy distribution through a variety of effects. First, any deviation from planarity in either the ground grid or the reflecting plate will lead to an inhomogeneous reflecting electric field. This will introduce some energy discrimination, since the low-energy metastable ions are more likely to be affected than would those produced by prompt ionization, which have a higher kinetic energy. This effect can arise due to the inability to produce perfectly planar fine wire mesh grids, such as the ground grid that serves as the gound potential at the entrance (and exit) of the ion reflector. Since the field here is nominally 600–700 V/cm, submillimeter deviations from planarity might produce a significant spread in the trajectory, and consequent time of arrival, of ions of different birth potentials. One possible method of reducing this effect is to increase the distance between the ground grid and the reflecting plate, but this introduces an undesirable "walk" or parallax in the ion beam, introducing an additional discrimination based on birth potential. A possible compromise is to reduce the diameter of the reflector to ensure better planarity of the wire grid, but again this must be balanced against the geometric constraints of the trajectory of the variable energy ion beam.

Finally, the regulation and measurement of the high voltages to the TOF lens and the ion reflector must be considered. Since

---

(7) Anderson, S. L.; Rider, D. M.; Zare, R. N. *Chem. Phys. Lett.* **1982**, *93*, 11.

(8) Durant, J. L., private communication.

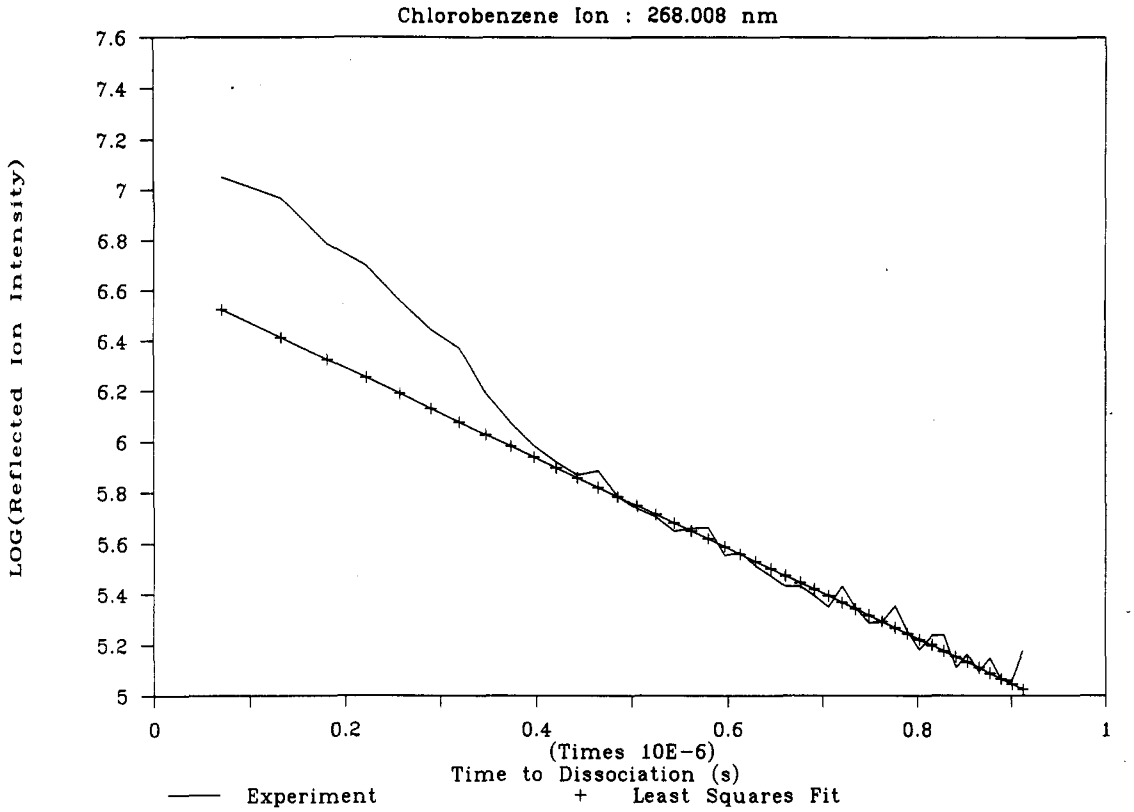

Figure 5. Analysis of ion reflector data. The parent plus daughter transmission curve is plotted against t_d, the time of dissociation. The derivation of t_d from the reflection potential and x_0 is found in the Theory and Analysis section. Also shown is a least-squares fit to the data. Note that the divergence on the data from the fit is a consequence of the nondissociating ion signal leaking into the integrated parent plus daughter ion signal, even though we are still below U_0, the birth potential. The rate constant from this plot is $k_{diss} = (1.78 \pm 0.09) \times 10^6\ s^{-1}$. The three-photon energy is 13.750 eV (268.005 nm).

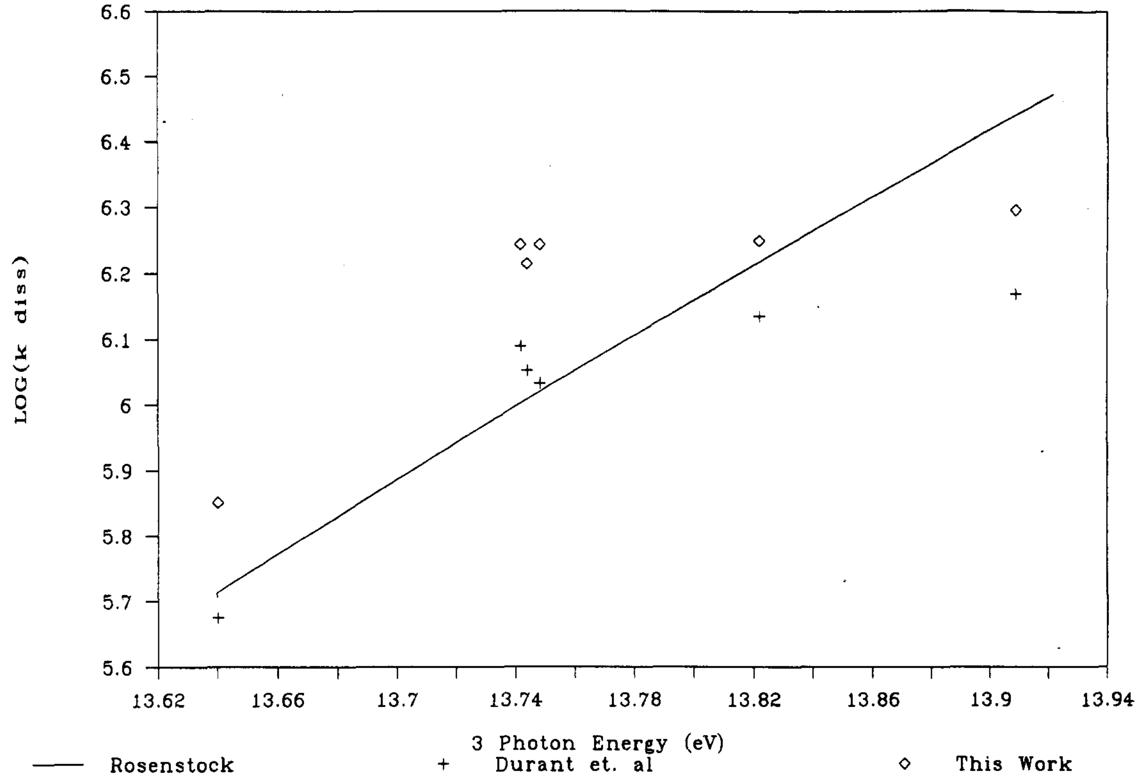

Figure 6. Unimolecular dissociation rate constants for $C_6H_5Cl^+$ plotted against three-photon energy. The energy is the sum of the energies of the three UV photons minus the photoelectron energy (3). The "+" represents the work of Durant et al.,[3] using a TOF tail distribution analysis. The solid line is the work of Rosenstock et al.,[2] who used the modified PIPECO technique by pulsing the extraction grids after a suitable delay and then fitted their "breakdown curves" to an RRKM model where all the transition state frequencies were reduced by 23%. Except for the point at 13.64 eV, where the error bars between our work and that of Durant et al. overlap, the error bars in the two sets of data are roughly the size of the plotted symbols.

all our measurements are referenced to ground, the accuracy of the voltage measurements must exceed 1 part in 10^5, or 0.001%. The regulation of the high-voltage power supplies is nominally within this accuracy, and the peak-to-peak ripple is below our sensitivity.

The rate constant data from Durant et al. are (on average) 30 (±5)% lower than the present work. While it is possible that instrument artifact is the explanation for this offset, the possibility exists that rotational excitation could be playing an important role in the measurement of the dissociation rate constant for $C_6H_5Cl^+$. A dependence of the rate of dissociation of the reaction $CH_4^+ \rightarrow CH_3^+ + H$ with rotational excitation was discussed by Illies et al.[9] In that work it was postulated that the observed rate constant was a result of quantum mechanical tunneling of the H atom through a centrifugal (rotational) barrier. However, the Cl atom tunneling is unlikely to be important in the dissociation reaction probed herein.

The recent work by Kiermeier et al.[10] and Neusser,[4b] on the unimolecular decay of benzene cation, have demonstrated that the metastable decay of J state-selected $C_6H_6^+$ ions show a marked dependence on J. By the use of a supersonic molecular beam and an effusive source, coupled with a narrow-band excitation laser ($\Delta\nu = 0.04$ cm^{-1}), they could generate J-selected neutral benzene molecules through the 6^0_1 rovibronic state. The J-selected S_1 state molecules were subsequently ionized by a second photon from the same narrow-band laser to generate benzene ions which retained their J selection. They investigated the range above the dissociation threshold from 1.2 to 1.6 eV by pumping the ion with a second laser. Their results show that a 30% decrease in the metastable dissociation rate constant was observed as $J \rightarrow 2$ to 58 (~5–300 K).

To model these results, they modified RRKM to include K, the projection of J onto the principal axis of the rotator, in the density of states, $\rho(E,J)$.[4b,10] They found that for K mixing, probably due to Coriolis coupling, and $K \leq J$ ($K = J, \ldots 0, \ldots J$) that $\rho(E,J) > \rho(E,0)$, assuming a tight activated complex. Since $k_{\text{diss}} \propto 1/\rho(E,J)$, then an increase in J would increase the density of states, which would lead to a decrease in the dissociation rate constant. Their calculations also show that a similar but smaller effect on k_{diss} is to be expected in the case of no K mixing. Finally, a larger effect of J on k_{diss} is postulated for a loose activated complex.

If these results are to bear upon the offset in the two data sets presented here, there must be some evidence of different rotational temperatures of the C_6H_5Cl in the jet between the two experiments. Both backing pressures and gas composition were the same in both setups. However, the nozzle used in the Durant experiments was a 500-μm-diameter pinhole as compared to a 750-μm-diameter conical nozzle used for our experiments. Since cooling in a supersonic jet goes as P_0D, where P_0 is the backing pressure and D is the nozzle diameter, we can expect that for the same pressure, our beam would result in ~50% better cooling. Harder to quantify is the effect of the conical nozzle, though it is known that a conical nozzle promotes greater cooling than a sonic nozzle.

Further evidence of a difference in the rotational energy distribution in the two experiments is seen in the agreement of the work of Ripoche et al.[11] with that of Durant et al. Ripoche et al. used a one-color two-photon absorption in C_6H_5Cl to make the chlorobenzene cation. A subsequent photon of different color from a second laser created the metastable ion. The dissociation rate constant, k_{diss}, was measured by tail-shape analysis of the metastable peak, as in the work of Durant et al. They found that they were in "excellent agreement" with the experiment of Durant et al. However, they used an *effusive* (*room temperature*) *beam* as the source of chlorobenzene neutrals.

Thus it might very well be that the lower rate constants measured by Durant (and Ripoche) are the result of rotationally hotter ions. The magnitude of the offset seems rather large, given that there was obviously considerable cooling in the Durant experiment. Interestingly enough, Rosenstock et al. consider that the activated complex of the dissociating chlorobenzene cation is loose.[2] If this were the case, then, as pointed out by Neusser,[4b] this would lead to an even larger effect as predicted by their modified RRKM model calculations. It may well be that the combination of a moderate difference in the rotational cooling of the two samples, along with the looseness of the activated complex, bring about the observed discrepancy.

The question of whether the ions produced by MPI are truly state selected comes up with regard to the lack of agreement of both this work and that of Durant et al. with the RRKM-fit data of Rosenstock et al. In the work of Ripoche,[11] which is in excellent agreement with Durant, all the metastable ions come from the ground state of the chlorobenzene ion at $\lambda = 269.887$ nm. Anderson et al.[7] have shown that there is essentially only one vibration excited in the ion by this 1 + 1 ionization process. Thus, the agreement cannot be the result of a difference in vibrational state selection. This must also be true for our work as well, since we agree well with Durant in the functional form of the k_{diss} versus energy.

Conclusions

The use of a simple one-stage ion reflector energy analyzer coupled with TOFMS provides a new and useful method for measuring unimolecular dissociation lifetimes in the 10^{-5}–10^{-7}-s range at the current acceleration potentials, as demonstrated by the good agreement between our results and those of the literature. With suitable changes in acceleration potentials, rates outside this range should become accessible and, with further refinements, even better precision can be anticipated.

Acknowledgment. Financial support by the U.S. Department of Energy, Grant No. DE-FG02-88-ER60648, is gratefully acknowledged. We thank R. N. Zare for helpful comments concerning the possible role of rotational effects and Paul Scheier for his 3-D graphics software.

---

(9) Illies, A. J.; Jarrold, M. F.; Bowers, M. T. *J. Am. Chem. Soc.* **1982**, *104*, 3587.

(10) Kiermeier, A.; Kühlewind, H.; Neusser, H. J.; Schlag, E. W.; Lin, S. H. *J. Chem. Phys.* **1988**, *88*, 6182.

(11) Ripoche, X.; Dimicoli, I.; LeCalvé, J.; Piuzzi, F.; Botter, R. *Chem. Phys.* **1988**, *124*, 305.